Rainfall-Induced Landslides: mechanisms, monitoring techniques and nowcasting models for early warning systems

Editors

L. Picarelli
Centro Interdipartimentale di Ricerca in Ingegneria Ambientale, Seconda Università degli Studi di Napoli

P. Tommasi
Istituto di Geologia Ambientale e Geoingegneria, C.N.R., Roma

G. Urciuoli
Dipartimento di Ingegneria Idraulica, Geotecnica ed Ambientale, Università degli Studi di Napoli Federico II

P. Versace
Dipartimento di Difesa del Suolo, Università degli Studi della Calabria

Failure modes and mechanisms in cohesive slopes: theoretical and numerical analysis of field and laboratory-triggered events

A. Spickermann & J.-P. Malet
School and Observatory of Earth Sciences, Institute of Earth Physics, CNRS UMR 7516, University of Strasbourg, Strasbourg, France

Th.W.J. van Asch
Faculty of Geosciences, Department of Physical Geography, Utrecht University, Utrecht, Netherlands

ABSTRACT: A basic requirement in landslide forecasting, quantitative risk assessment and management (e.g. design of early warning systems) is the identification and modelling of failure modes and triggering mechanisms. This work focuses on the analysis of slope failure that take place in cohesive soils, such as reworked clay-shales. First, failure modes in cohesive slopes are presented and analysed theoretically using field observation (case study of the Super-Sauze mudslide) and laboratory experiments (small-scale landslides triggered in a flume). Second, the presented observations are analysed numerically by means of the 2LM, landslide liquefaction model, a simple analytical model based on the method of limit equilibrium. Possible failure modes, triggering mechanisms and tentative modelling are discussed.

1 INTRODUCTION

A landslide can show a variety of failure modes which depends on the given conditions of the slope such as geometry, material characteristics and presence of discontinuities. Besides the gravity as main loading factor, it is assumed that slope failures are often caused by hydrological processes. The identification and modelling of failure modes and triggering mechanisms are essential requirements in landslide forecasting and in the design of reliable early warning systems.

Failure can occur as a series of multiple slide events, i.e. retrogressively, or as complete flowslide, associated with liquefaction, the behaviour of soils that go from a solid to a liquefied state which is related to an increase in pore water pressure and consequently a decrease in shear strength, i.e. reduction in effective stress. Failure can also occur as translational or rotational movement along a single shear surface, as progressive failure. Slope movements can vary between gradual deformation and rapid run-out. The mechanisms leading to typical failure modes are often uncertain and difficult to explain. For example in van Asch et al. (2006) and van Asch & Malet (in prep.) several mechanisms which may generate liquefaction and the corresponding literature references are summarized. Progressive failure requires a shear zone undergoing a transition between peak and residual strength (Bjerrum, 1967). The growth of a shear surface is accompanied with the loss of shear resistance or the degradation of shear parameters such as friction angle and cohesion (softening). Eberhardt et al. (2004) investigate the concept of progressive failure and the numerical modelling of rock mass strength degradation in natural rock slopes using the Randa rockslide. Petley et al. (2005) present a model for the growth of landslide shear surfaces, and hence for progressive failure, based upon laboratory testing of materials under conditions that simulate those within a hydrologically-triggered landslide, i.e. conventional isotropic consolidation and undrained shear tests. By now almost all of the experimental studies have been performed on clean sands, i.e. little work has been performed on silt and silt-clay mixture (Wang & Sassa, 2003). But despite numerous studies which have been done there is still uncertainty in the explanation of the processes determining the failure.

This study is an attempt to get a better understanding of the mode of failure and possible failure mechanisms taking place in cohesive slopes. Theoretical analysis has been carried out on the basis of (1) field observations of two failure events of the clay-rich Super-Sauze mudslide (Southeast France) and (2) small-scale landslides triggered in a flume using clay from Zoelen (Netherlands) and reworked black marls from Super-Sauze.

To investigate the failure behaviour numerically a simple analytical model, named 2LM (Landslide Liquefaction Model) (van Asch et al. 2006; van Asch & Malet, in prep.) is used. By means of this model the development of excess pore water pressure and possible liquefaction can be studied taking into ac-

count the effects of landslide geometry and kinematic deformation. Results from an application of this model on the two slump-type failures that occurred in the Super-Sauze mudslide are presented. Then the model is applied to the flume experiments.

Finally, tentative modeling is discussed and the observed failure modes and possible mechanisms leading to failure are summarized.

2 FIELD OBSERVATION - THE SUPER-SAUZE MUDSLIDE

One example of a landslide occurring in cohesive material is the Super-Sauze mudslide (Southeast France) consisting of reworked and loosely packed clay-rich material (i;e. black marls). It is used to describe possible failure modes and potential failure mechanisms of cohesive slopes observed in the field. The Super-Sauze mudslide is extensively investigated in several studies, e.g. Malet (2003), Malet et al. (2005) and Maquaire et al. (2003). It is located in the headwater basin of the Sauze torrent watershed (a tributary of the Ubaye river) between 2150 (crown) and 1740 m (toe) for an average slope of 25°. It covers a 0.17 km² surface with a length of 0.8 km and a maximum width of 0.2 km for a thickness ranging between 8 and 20 m. The mudslide is characterized by a complex style of activity associating continuous slow movement of 0.002 to 0.03 m.day^{-1}. In this work, two slump-type failures, which developed in secondary scarps on the upper parts of the Super-Sauze mudslide in 1999 and 2006 are presented.

The first slump (1999) started as rotational slide, but acquired flow characteristics very quickly. All the material disappeared from the source area and completely liquefied into a mudflow. The mean gradient of the slip surface is assumed to be around 46° (Fig. 1a). The calculated velocity of the slump reaches a peak value of 5.1 m.s^{-1} (Malet et al. 2003) and can be described as very rapid. Field observations suggest that the initial movement was of the slump type, what means that failure starts with the development of a sliding surface followed by a flow, i.e. by liquefaction of the failure mass.

The second slump (2006) did not liquefy and the slumped material remained for a large part in the source area. A pre-failure and a post-failure topography have been reconstructed from a DGPS survey (Fig. 1b). The mean gradient of the slip surface is estimated at ca. 28°.

Malet (2003) and Malet et al. (2005) state that these slumps occurred through a combination of heavy and sustained rainfalls, thawing soils and snowmelt. When interpreting failure mechanisms of the slump events, the whole Super-Sauze mudslide is included.

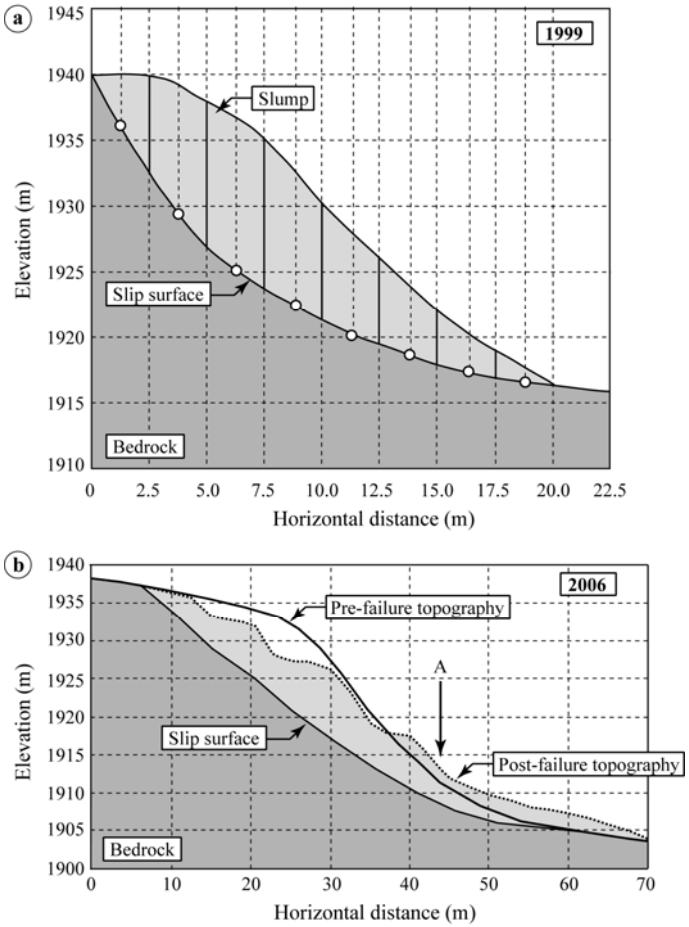

Figure 1. Schematic cross-sections of the slump-type failures of 1999 (a) and 2006 (b) at the Super-Sauze mudslide.

Mechanisms leading to the total mudslide movement and to secondary failure events are assumed to be:

– internal creep effects in relation to seasonal changes in pore water pressures,
– acceleration in relation to local lateral compression of the material during motion, undrained loading and the development of excess pore water pressures.

3 LABORATORY OBSERVATION - FLUME EXPERIMENTS

Simple small-scale landslides are triggered in the laboratory by means of flume experiments to get a better understanding of the failure behaviour of cohesive slopes. Tests using two different kinds of cohesive materials (clay from Zoelen, the Netherlands; reworked clay-rich material from Super-Sauze, France) are carried out. The grain size distributions are given in Figure 2.

3.1 *Flume test apparatus and test procedure*

The test apparatus is depicted in Figure 3. The inner dimensions of the flume are 250 cm in length, 60 cm in height and 60 cm in width. The flume angle α is made changeable for different test requirements.

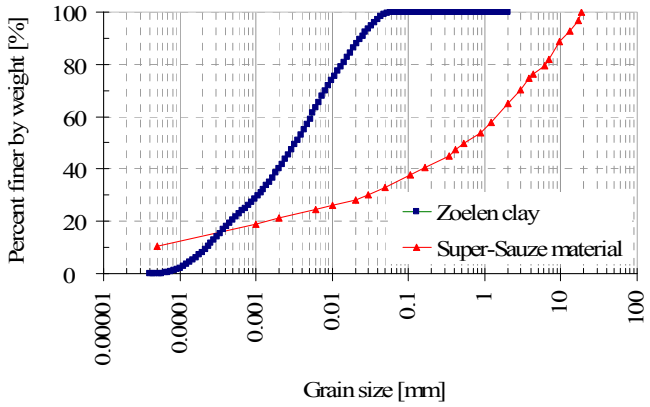

Figure 2. Grain size distributions of the tested material.

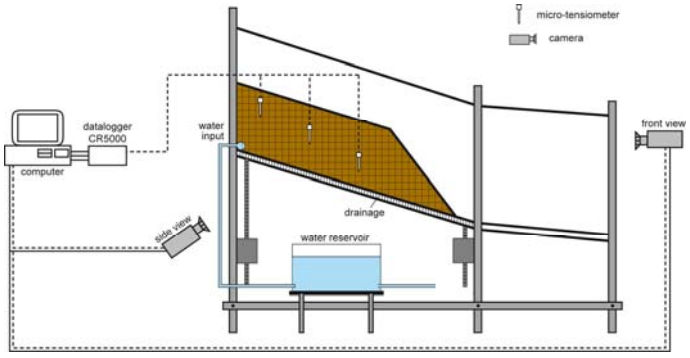

Figure 3. Scheme of the flume device.

The test apparatus consists of one transparent side. Images are taken in defined intervals from this side and from the front. Displacements fields are computed from correlation of multi-temporal optical images (CIV). Pore water pressure is monitored by tensiometers. The tensiometers consist in piezoresistive pressure transducers (Keller©) mounted on a ceramic cup of 6 mm in diameter. To investigate the hydrological trigger, water infiltrates from the back bottom of the slope using a pump and a defined top water level that is kept constant (upward constant head infiltration).

3.2 *Analysis of flume test on Zoelen clay*

The first experiment is carried out on Zoelen clay. Before the slope was built the material was saturated in buckets what leads to a strong compacted slope with a height of 40 cm, a width of 60 cm, a length of 57 cm and a slope angle of 35° with respect to a horizontal flume surface ($\alpha = 0°$). The flume was tilted back with a flume angle of -21° (26-09-08), that gives a total slope angle of $\gamma = 16°$. After three days of drying, water infiltration was started (29-09-08). After another two days, the flume was tilted to $\alpha = 11°$ (01-10-08), which gives a total slope angle of $\gamma = 46°$. Final failure occurred after additional three weeks of water supply (24/25-10-08).

Displacements in time are measured using two points at the slope surface (Fig. 4). Figure 5 presents the time displacement curves of the whole failure process (25 days). From 01-10-2008 until 24-10-2008 only very slow movements took place. Displacements of that period are about 5 mm. Then the movement velocity increases and final failure occurs. The time displacement graphs of the final failure (Fig. 6) indicate that final failure takes place in two stages, both on the 25-10-08, the first between 0:28 and 03:24 and the second between 5:20 and 7:20.

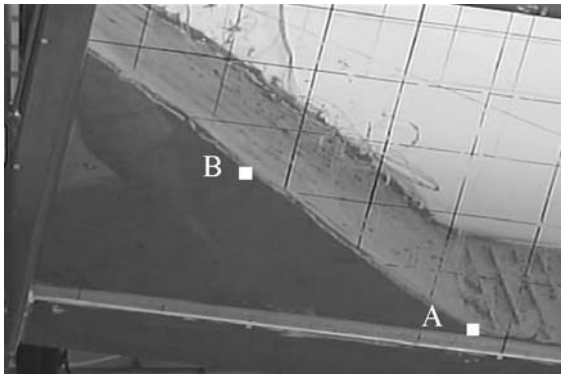

Figure 4. Initial test conditions and observed points of the flume test on Zoelen clay.

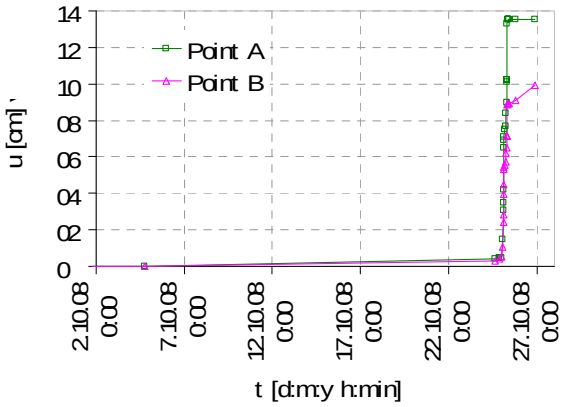

Figure 5. Time displacement curves of two points at the slope surface of the flume test on Zoelen clay.

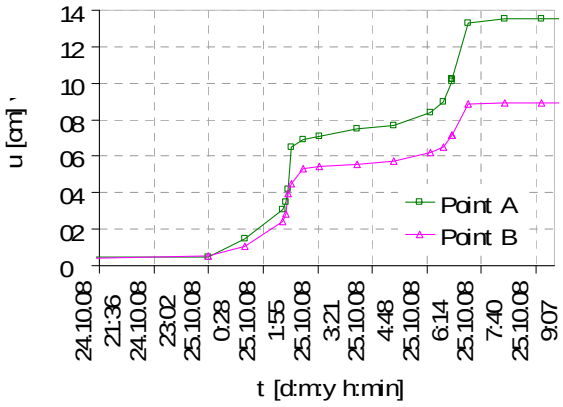

Figure 6. Time displacement curves of the last phase of failure of the flume test on Zoelen clay.

Even if the movement along the slip surface in this phase is faster than the movement before the 25-10-08 it can be described as rather moderate. Figure 7 shows the slope after failure on the 26-10-2008 including the final positions of the observed

points A and B. The whole failure process lasts about three weeks.

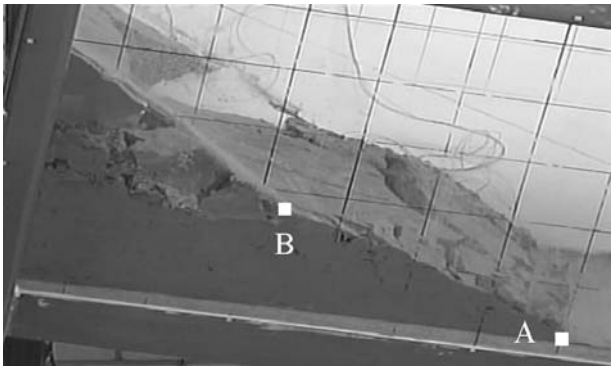

Figure 7. Slope after failure, 26-10-2008, inclusive final positions of observed points A, B of the test on Zoelen clay.

Pore water pressure measurements are taken at nine locations from the cross section in the centre of the slope (Fig. 8). Figure 9 gives the pore water pressures *p* measured during the time of final failure. Tensiometers T2, T3 and T6 show a small response to the two stages of failure (Fig. 6). It can be summarized that almost no excess pore water pressure is generated during motion along the slip surface. Pore water pressure measurements of the whole experiment which are not given here indicate that only tensiometers T1 and T2 show positive values. An increase of positive pore water pressures is not observed and can be excluded as possible triggering mechanism.

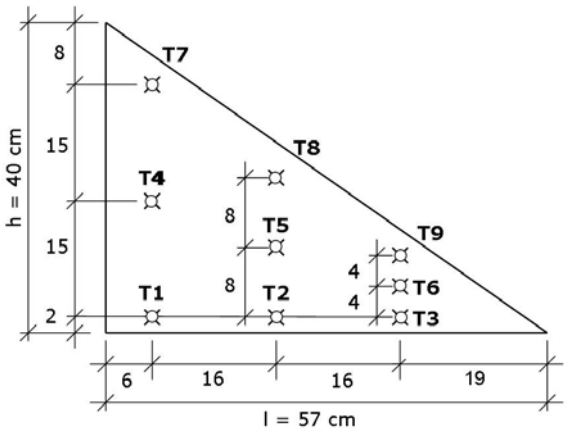

Figure 8. Position of tensiometers in the middle cross section of the slope consisting of Zoelen clay.

The first part of the failure process before 25-10-08 is characterised by the development of fissures and cracks. It is assumed that these cracks develop because of desiccation. This phase can be described by the initialization of failure, i.e. the formation and the growth of a completely developed shear surface. The second phase contains the movement of the soil mass along the developed shearing zone. Final failure occurs within one slump in two stages. The whole process is characterised as progressive failure.

In general it is assumed that progressive failure is caused by the decrease of shear resistance, i.e. the reduction of shear parameters, as friction angle and cohesion. According to Petley et al. (2005) the small displacements in the first part of the failure process are caused by microcrack formation. Even if the microcracks weakens the slope slightly it is still in a stable state. Shear surface formation starts when the microcrack density reaches the point at which interaction between them begins. Petley et al. (2005) propose that during this early phase of shear surface development, a reduction of pore pressure can stop the deformation.

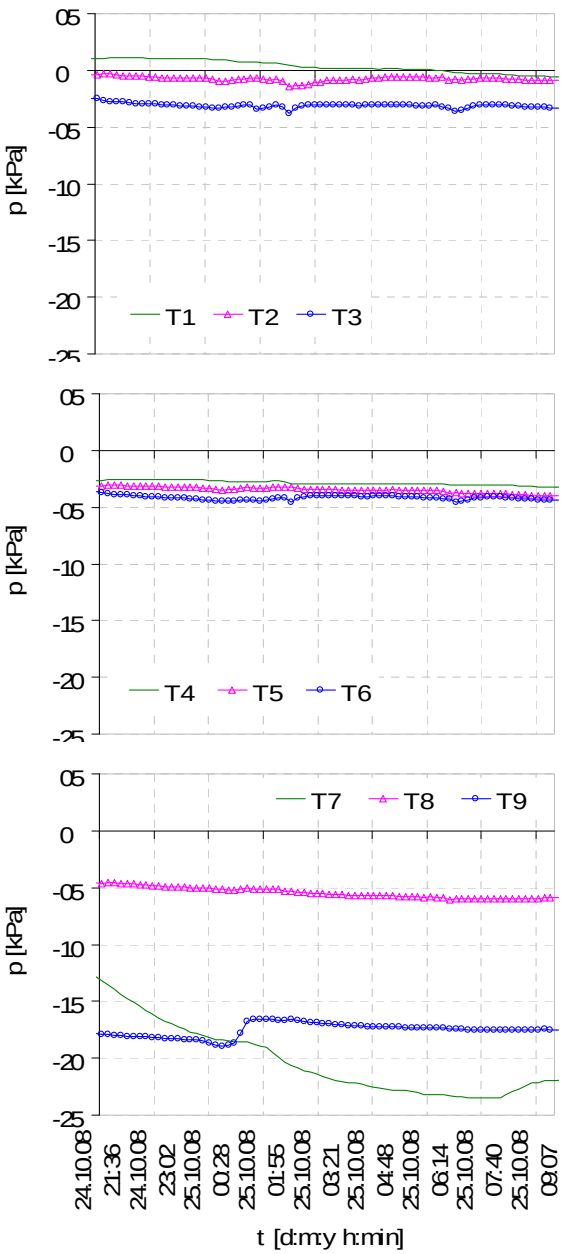

Figure 9. Pore water pressure measurements of tensiometers T1, T2 and T3 during final failure of the flume test on Zoelen clay.

One can conclude that the constant water supply in the flume experiments supports the development of microcracks and further the formation of a slip surface. The acceleration to failure in the time displacement curve starts when shear stress exceeds

shear strength. From this point pore pressures become increasingly unimportant for the deformation.

3.3 *Analysis of flume test on Super-Sauze material*

The second experiment is carried out on loosely packed material from Super-Sauze. Slope dimensions are 23 cm in height and 90 cm in length. Water infiltration has started with a horizontal flume surface on the 13-03-2009. The flume inclination has been increased gradually to a value of 18° till the 18-03-2009 (16:00), that leads together with the slope angle of about 14° to a total slope angle of about 32°.

On the 18-03-2009 at 21:45, failure starts at the toe at the right side of the flume as seen from the front and it continues in direction of the crest. In Figure 10, the development of slumps is displayed. Failure occurs in sudden multiple superficial sliding with a subsequent slow movement of the whole failure mass. The total time span of failure is about 8 hours. The total failure process can be defined as retrogressive slumping. However the behaviour at the beginning of failure is not clearly identified. It is supposed that due to liquefaction at the toe, a first slip surface (slump 1) is formed. The following mechanisms are considered to be possible reasons for the liquefaction in the performed flume experiment:

- occurrence of seepage flow, with a water flow gradient that is approximately opposite to the direction of gravity force causing decrease of effective stress,
- natural porosity of the soil is near liquid limit,
- compression at the toe leads to excess pore water pressures (i.e. decrease of effective stress).

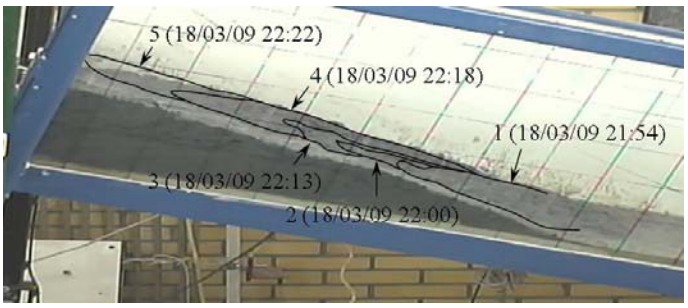

Figure 10. Final state of flume experiment on material from Super-Sauze with retrogressive development of slumps.

4 LANDSLDE LIQUEFACTION MODEL

A simple analytical model, named 2LM (Landslide Liquefaction Model) is developed to study the generation of excess pore water pressure and possible liquefaction of sliding blocks (van Asch et al. 2006). The model assumes that liquefaction is related to previous development of slip surfaces, i.e. deformation of the landslide body (sliding blocks, slumps) during motion leading to the generation of excess pore water pressure and thus to liquefaction. The model is based on the theory of limiting equilibrium dividing the area above an estimated slip surface into slices of constant width. Immediately after failure, the difference in movement for each slice is calculated assuming a viscous shear band and using the Coulomb-viscous model. The differential movements conduct to differential strains which are transferred to excess pore water pressures. The potential liquefaction is then evaluated for each slice in relation to the displacements.

4.1 *Application to Super-Sauze slumps*

In van Asch et al. (2006) and van Asch & Malet (in prep.), the model is applied to the dataset available for the two slump-type failures that occurred on the Super-Sauze mudslide (Fig. 1). Table 1 gives the material parameters used in the 2LM calculations.

Table 1. Material parameters used in the 2LM model of the Super-Sauze slumps.

Friction angle, φ [°]	32
Cohesion, c [kPa]	14
Young's modulus, E [kPa]	$3.2*10^{4}$
Consolidation coefficient, C_v [m²/s]	$6.36*10^{-7}$
Skempton's pore pressure coefficient, A [-]	0.5
Dynamic viscosity, η [kPa s]	$1.21*10^{+3}$ *
	$7.41*10^{+6}$ **

* slump 1999, ** slump 2006.

In Figure 11 the development of pore water pressure during motion of the slump in 1999 is depicted. A pore pressure ratio equal to unity implies that the effective stress between grains is zero and the material liquefies. Figure 11 shows the successive liquefaction of the slices in the lower part of the moving mass in relation to the mean displacement of the slump. Once a displacement of 0.07 m is reached, the two lowest slices (with a distance of 17.5 m and 15 m from the main scarp) liquefy. After a displacement of 0.48 m the material 10 m from the main scarp liquefies.

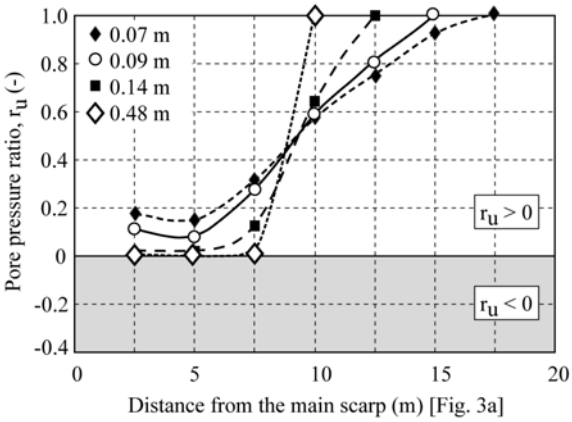

Figure 11. Development of pore water pressures in the slices of the failure body (identified through the distance from the main

scarp) in relation to the mean displacement of the Super-Sauze slump in 1999.

In contrast to field observations that showed a nearly complete liquefaction of the whole failure mass (Malet et al. 2005) the calculation indicates that about half of the slumping mass liquefies.

In van Asch et al. (2006) it is hypothesized that the stabilisation of the remaining part caused by the calculated decrease in pore pressure towards zero adds too much strength and, hence, too much stability. Decrease in pore water pressure may rapidly vanish or may not be generated in the dilatation zone due to the formation of fissures. That means that the upper part under more neutral pore water pressure conditions still could move further downwards, deform and partly liquefy.

Figure 12a gives the comparison of the observed and simulated post-failure topography of the 2006 slump.

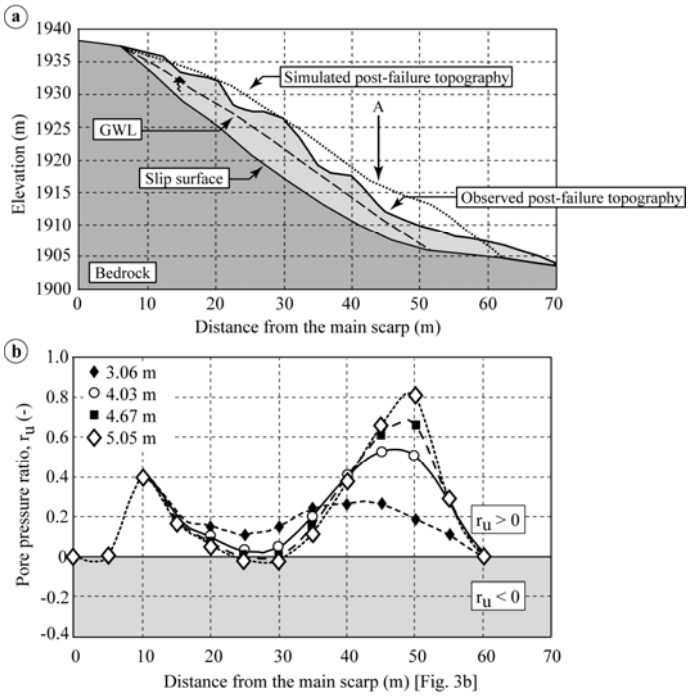

Figure 12. 2LM calculation of the Super-Sauze slump in 2006; (a) observed and simulated post-failure topography, (b) development of pore water pressures in the slices of the failure body (identified through the distance from the main scarp) in relation to the mean displacement of the moving mass.

One reason for the difference between observed and calculated topography is the simple geometry of the slip surface given as input condition in the 2LM. The realistic slip surface is supposed to be more irregular. In Figure 12b the development of pore water pressure in relation to the displacement of the sliding mass at all slice locations measured from the main scarp is shown. The slump stopped after a movement of 5.1 m without liquefaction. The relative high pore pressure ratio at the toe may explain some weakening and larger run-out distances than modelled.

4.2 *Application to flume experiment on Zoelen clay*

Even if failure observed in the flume experiment on Zoelen clay proceeds progressively without liquefaction, the 2LM can be used to simulate the deformation of the landslide body since it solves the equations of limit equilibrium. Material parameters used in the calculation are displayed in table 2. The cohesion in the slip surface is set almost to zero, which corresponds to the assumption that progressive failure takes place in consequence of the reduction of shear resistance. The generation of excess pore water pressure due to the development of a slip surface and associated liquefaction has apparently no relevance in this failure process.

Table 2. Material parameters used in the 2LM model of the flume experiment on Zoelen clay.

Friction angle, φ [°]	35
Cohesion, c [kPa]	0.01
Young's modulus, E [kPa]	$1.2*10^{3}$
Consolidation coefficient, C_v [m²/s]	$9*10^{-6}$
Skempton's pore pressure coefficient, A [-]	0.6
Dynamic viscosity, η [kPa s]	$8*10^{+3}$

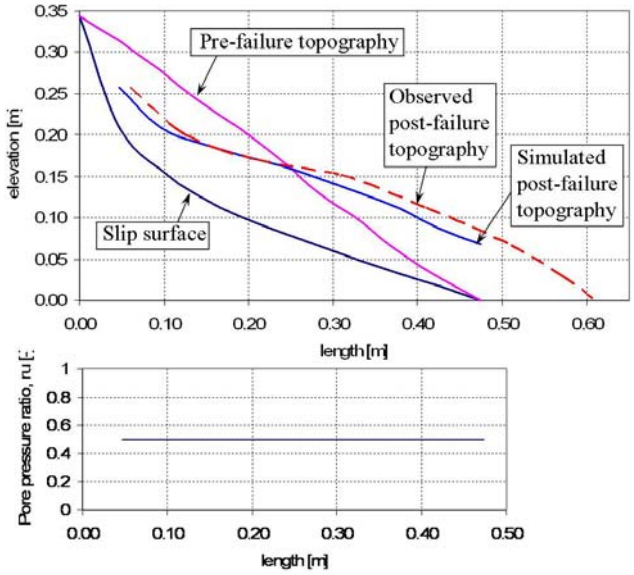

Figure 13. 2LM calculation of the flume experiment performed on Zoelen clay; (a) observed and simulated post-failure topography, (b) pore pressure ratio in the failure body.

To exclude the development of a pore pressure ratio equal to unity (i.e. resulting in liquefaction), the consolidation coefficient is enlarged.

The comparison between observed and simulated post-failure topography (Fig. 13) shows a good agreement. The pore pressure ratio r_u is equal to a constant value of 0.5.

4.3 *Application to flume experiment on Super-Sauze material*

The failure mode observed in the flume experiment on Super-Sauze material is characterized as retro-

gressive slumping with foregoing liquefaction at the toe. In opposite to the observation, the 2LM assumes that first a slip surface has to develop before the material can liquefy. Still the 2LM is used to analyse the failure process. Table 3 contains the material parameters. Shear parameters, cohesion and friction angle correspond to residual values. In Figure 14, a comparison between observed and simulated post-failure topography and the pore pressure ratio at the end of the failure process are displayed.

Table 3. Material parameters used in the 2LM model of the flume experiment on material from Super-Sauze.

Friction angle, φ [°]	16 (7 *)
Cohesion, c [kPa]	0.01
Young's modulus, E [kPa]	$1*10^{3}$
Consolidation coefficient, C_v [m²/s]	$5*10^{-7}$
Skempton's pore pressure coefficient, A [-]	0.5
Dynamic viscosity, η [kPa s]	$1.1*10^{+3}$

* apparent friction angle.

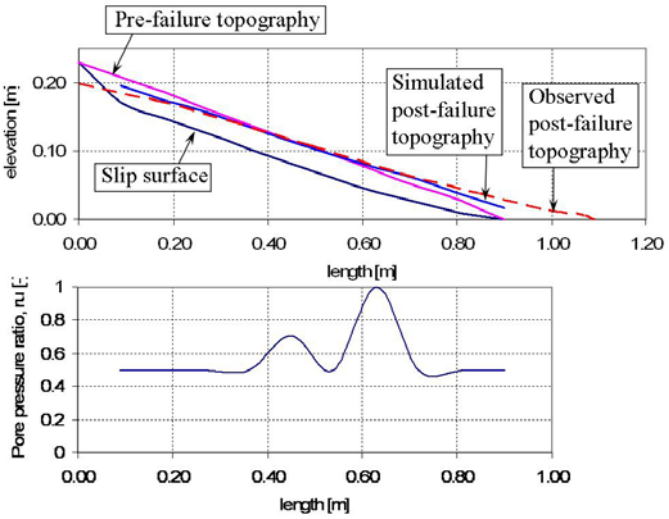

Figure 14. 2LM calculation of the flume experiment performed on reworked material from Super-Sauze; (a) observed and simulated post-failure topography, (b) pore pressure ratio in the failure body.

To reproduce a post-failure surface similar to the observed post-failure surface, the friction angle has to be reduced. The graph of the pore pressure ratio suggests that the material about 60 cm from the main scarp of the slip surface liquefies. The calculation reproduces the real failure process very simplified because the retrogressive development of slumps is summarized in one slip surface. It has to be proofed if the analysis of single slumps gives more realistic results.

5 TENTATIVE MODELLING

The 2LM model can be used only for a very rough interpretation of the failure behaviour. If no liquefaction is involved in the failure process, a pure limit equilibrium analysis is performed. The model presumes that a movement of the landslide along a slip surface leads to the generation of excess pore water pressure and thus to liquefaction. This interpretation covers only one possible failure mechanism. For example, seepage can be analysed by coupled hydro-mechanical finite element modelling (Zhang et al. 2005) since seepage and stress-deformation problems are strongly linked. Pore water pressure changes due to seepage lead to changes in stresses and therefore to deformations of the material. Conversely, stress changes modify the seepage process because soil hydraulic properties such as porosity, permeability and water storage capacity are affected by the changes in stresses.

To model phenomena as progressive failure, more appropriate numerical methods are required. The flume experiment on Zoelen clay will be simulated using the FEM, finite element method. The development of a sliding surface can be taken into account through an adequate material approach. For example Eberhardt et al. (2004) use an elasto-plastic material model in which strength degradation is considered by introducing the strength to be a function of strain. Forlati et al. (2001) take into account non-linear, time-dependent behaviour in the analysis of a slope in Rosone (Italian Alps) using an isotropic, elastic-viscoplastic constitutive law, allowing for strain softening. In Spickermann (2008) shear plane development is simulated by an elastic-viscoplastic material model with hardening and softening. Hardening and softening is introduced in the constitutive law in terms of mobilized shear parameters which are functions of the equivalent viscoplastic strain.

6 CONCLUSIONS

The theoretical and numerical analysis of failure modes and failure mechanisms carried out on two slump events of the clay-rich Super-Sauze mudslide and two small-scale landslides triggered in flume experiments on clay from Zoelen and on material from Super-Sauze leads to following results. The failure behaviour of cohesive slopes can show extreme different modes, varying between liquefaction, retrogressive failure and progressive failure that are related to different failure mechanisms.

The observed failure that occurs within the Super-Sauze landslide in 1999 is described as flow-like phenomena that starts with sliding and ends up in a nearly complete liquefaction. The lateral compression of the material during motion of the whole landslide, undrained loading and the development of excess pore water pressures are indicated as possible failure mechanisms. The 2LM can not reproduce complete liquefaction and predicts liquefaction of about 50% of the sliding mass. The stabilisation of the remaining part caused by the calculated decrease

in pore water pressure towards zero adds too much strength and, hence, too much stability.

The second failure in 2006 is characterized as slump without any liquefaction. Mechanisms leading to failure correspond to those of the slump in 1999. A comparison of the observed and simulated post-failure topography obtained from the 2LM analysis shows irregularities that can be certainly ascribed to the simple slip surface used in the calculation which does not correspond to the realistic slip surface. The modelling confirms the observation that no liquefaction takes place.

The flume experiment on Zoelen clay shows failure initialized over a long time period and occurring progressively. After a shear surface is formed the soil slumps down along the surface in several stages, with different velocities, that could be related to a renewed building up of pore water pressure in opening fissures. Failure takes place without any liquefaction. Mechanisms leading to progressive failure are related to the reduction of shear resistance of the material. According to Petley et al. (2005) shear surface growth starts with microcracking. After point interaction and coalescence of microcracks is achieved further shear surface development leads to stress concentration and acceleration of sliding movements. Since no excess pore pressure is measured in the experiment liquefaction has no meaning in this failure process, what means that the 2LM is used to perform a pure limit equilibrium analysis. The observed and calculated post-failure topography are in a good agreement.

The experiment performed on the Super-Sauze material shows a failure mode completely different from the test on Zoelen clay. It can be described as retrogressive failure that proceeds as a series of multiple slide events. It is observed that failure starts at the toe with liquefaction. The mechanisms leading to liquefaction are not clearly indicated. Possible explanations could be the seepage forces caused by the infiltration of water or that the material is near the liquid limit. The assumption that due to liquefaction of the soil at the toe, the first slip surface is formed is contrary to the hypothesis used in the 2LM that liquefaction requires first the forming of a slip surface.

More sophisticated modelling, as finite element modelling is necessary to reproduce the slope behaviour more realistically. To simulate progressive failure softening effects in the material approach can be used.

ACKNOWLEDGMENTS

This work is supported by the European Commission under the Marie Curie Research and Training Network '*Mountain Risks: from prediction to management and governance*' (MCRTN-035798) and by ANR (France) under contract TriggerLand '*Triggering Mechanisms of Landslides*' (ANR-06-CATT-011).

We thank M.C.G. van Maarseveen, D.B. van Dam and H. Markies for the technical support in the laboratory experiments.

REFERENCES

Bjerrum, L. 1967. Progressive failure in slopes of overconsolidated plastic clay and clay shales. Journal of the Soil Mechanics and Foundations Division of the American Society of Civil Engineers 93: 1-49.

Eberhardt, E., Stead, D. & Coggan, J.S. 2004. Numerical analysis of initiation and progressive failure in natural rock slope - the 1991 Randa rockslide. International Journal of Rock Mechanics & Mining Sciences 41(1): 69-87.

Forlati, F., Gioda, G. & Scavia, C. 2001. Finite Element Analysis of a Deep-seated Slope Deformation. Rock Mechanics and Rock Engineering 34(2): 135-159.

Malet, J.-P. 2003. Les "glissements de type écoulement" dans les marnes noires des Alpes du Sud. Morphologie, fonctionnement et modélisation hydro-mécanique. PhD Thesis, Univ. Louis Pasteur, Strasbourg, France, 394p.

Malet, J.-P., Remaître, A., Maquaire, O. & Locat J. 2003. Dynamics of distal debris-flows induced in clayey earthflows. Implications for hazard assessment. In Picarelli, L. (Ed): Proceedings of the International Conference on Fast Slope Movements: Prediction and Prevention for Risk Mitigation. Napoli, Italy, Patron Editore, Bologna, 341-348.

Malet, J.-P., Laigle, D., Remaître, A. & Maquaire, O. 2005. Triggering conditions of debris-flows associated to complex earthflows. The case of the Super-Sauze earthflow (South Alps, France). Geomorphology 66(1-4): 215-235.

Maquaire, O., Malet, J.-P., Remaître, A., Locat, J., Klotz, S. & Guillon, J. 2003. Instability conditions of marly hillslopes: towards landsliding or gullying? The case of the Barcelonnette Basin, South East France. Engineering Geology 70(1-2): 109-130.

Petley, D.N., Petley, D.J., Bulmer, M.H. & Carey, J. 2005. Development of progressive landslide failure in cohesive materials. Geology 33(3): 201-204.

Spickermann, A. 2008. Analyse tiefgreifender Hangdeformationen - Einfluss des Initialspannungszustands und der konstitutiven Formulierung. In: Schriftenreihe Geotechnik, no.18, Bauhaus-Universität Weimar.

Wang, G. & Sassa, K. 2003. Pore-pressure generation and movement of rainfall-induced landslides: effects of grain size and fine particle content. Engineering Geology 69: 109-125.

van Asch, Th.W.J., Malet, J.-P. & van Beek, L.P.H. 2006. Influence of landslide geometry and kinematic deformation to describe the liquefaction of landslides: some theoretical considerations. Engineering Geology 88: 59-69.

van Asch, Th.W.J. & Malet, J.-P. Fluidization potential of soils as an important aspect in landslide hazard analyses. submitted to Natural Hazards and Earth Systems Science.

Zhang, L., Zhang, L.M. & Tang, W.H. 2005. Rainfall-induced slope failure considering variability of soil properties. Geotechnique 55(2): 183-188.